J. of Electromagn. Waves and Appl., Vol. 25, 2138–2147, 2011

A BROAD-BANDWIDTH DUAL-BAND BANDPASS FILTER DESIGN USING COMPOSITE RIGHT/LEFT HANDED TRANSMISSION LINES

G. Chaudhary[1], Y. Jeong[1,*], and J. Lim[2]

[1]Division of Electronics and Information Engineering, Chonbuk National University, 664-14, Deokjin-dong, Deokjin-gu, Jeonju, Chonbuk 561-756, Republic of Korea

[2]Department of Electrical and Communication, Soonchunhyang University, Asan, Chungnam, Republic of Korea

Abstract—In this paper, a novel design of a dual-band bandpass filter (BPF) with a broad bandwidth and low insertion loss is presented. The proposed BPF consists of short-stub composite right/left handed transmission lines and dual-band admittance inverters. Both theory and experiment have been presented in order to validate the proposed structure. The proposed dual-band BPF has the 3-dB fractional bandwidths (FBWs) of 50.24% and 20.20% at center frequencies of 2.40 GHz and 5.20 GHz, respectively, useful for wireless local area networks applications. From the measured performance, the dual-band BPF has the low insertion losses of 0.28 dB and 0.46 dB for each passband and high isolation of 39.9 dB in between two passbands.

1. INTRODUCTION

In the rapid evolution of various wireless services, multi-band BPFs capable of adapting to multiple wireless communication platforms have seen their use increase considerably. Extensive studies on the design of multi-band BPFs can be found in literatures. The multi-band BPFs can be intuitively implemented by simply connecting several BPFs having different passbands in parallel [1–4]. However, these kinds of filters not only increase the overall BPF size, but also require additional combining matching networks at the input and output ports of the BPF.

Received 1 September 2011, Accepted 4 October 2011, Scheduled 11 October 2011

* Corresponding author: Yongchae Jeong (ycjeong@jbnu.ac.kr).

Applying two step frequency transformations to low pass prototype can achieve narrow dual passband capability BPF [5]. Recently, the multi-mode resonators such as stepped impedance resonators (SIRs), stub-loaded SIRs, meander-loop resonator and complement split-ring resonator (CSRR) defected ground structure have been widely used to design the dual-band BPFs utilizing higher resonant modes of resonators [6–14]. The resonant modes for SIR can be controlled by characteristic impedances of the high and low sections of resonators. However, these approaches have some difficulties in the adjustment of coupling coefficients between neighboring resonators to meet the dual-band specifications. Moreover, the above referenced filters have narrowband characteristics. Some efforts have been made to design broad-bandwidth dual-band BPF using SIR and slotted ground structures [15–18]. However, they require some complex and time consuming mathematical calculations to find the desired element values of filter.

The composite right/left handed (CRLH) meta-material transmission line (TL) is composite of the left handed (LH) and right handed (RH) TLs, which are widely used to design the dual-band microwave circuits such as couplers, power dividers, power amplifiers, etc. [19–22]. The dual-band characteristics of the CRLH TLs have also been used in the design of narrowband BPFs [23–25]. When designing broad-bandwidth BPFs, the structure must be different from narrowband BPFs. For broadband characteristics, the resonators having strong coupling or multi-modes are required [26, 27]. Therefore, the dual-band BPF having broad bandwidth and low insertion loss characteristics is a challenging work to filter designers.

In this paper, the design of dual-band BPF with broad-bandwidth characteristics is proposed. It utilizes the dual-band characteristics of short stub CRLH TLs. The couplings between resonators have been implemented with dual-band admittance inverters which consists of open stubs and transmission line connected in π-structure. The simple design equations are provided to find the element values of filter with given specification of filter. This paper is organized as follows. First, we provide the mathematical analysis of CRLH TLs and dual-band admittance inverters to design the dual-band BPF. Second, the simulation and experiment results are provided followed by conclusion.

2. DESIGN METHOD

Figure 1 shows a topology of the proposed broad-bandwidth dual-band BPF, which consists of short stub CRLHs and dual-band admittance inverters. The short stub CRLH shown in the figure usually exhibits

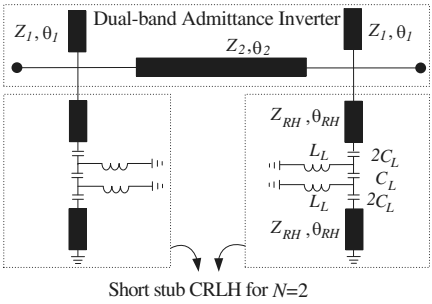

Figure 1. Proposed dual-band bandpass filter using dual-band resonators and admittance inverter.

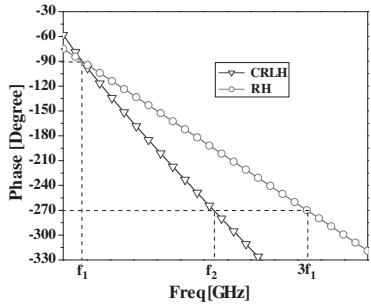

Figure 2. The simulated phase response of CRLH dual-band $\lambda/4$ and RH $\lambda/4$ transmission line.

interesting phase response characteristics as in Fig. 2. Due to the positive phase response of LH TL, the CRLH TL exhibits higher phase slope than the conventional RH TL for the same electrical length at the same fundamental frequency (f_1). In order words, the electrical length of odd multiple of $-90°$ ($\lambda/4$ and $3\lambda/4$) is obtainable at the odd harmonic frequencies in case of the RH TL. However, the frequency with $3\lambda/4$ wavelength, which is the second passband frequency, can be controlled by adjusting a number of LH unit cells (N) and element values of LH TL (C_L, L_L) together with the electrical length (θ_{RH}) of RH TL as shown in Fig. 2.

The design equations needed to find the element values of CRLH TL presented in [28] are given as:

$$L_L = \frac{NZ_{\mathrm{RH}}\left[1-(\omega_1/\omega_2)^2\right]}{\omega_1\left[\phi_1-\phi_2\left(\omega_1/\omega_2\right)\right]} \tag{1}$$

$$C_L = \frac{N\left[1-(\omega_1/\omega_2)^2\right]}{\omega_1 Z_{\mathrm{RH}}\left[\phi_1-\phi_2\left(\omega_1/\omega_2\right)\right]} \tag{2}$$

$$\phi_i^{\mathrm{RH}} = -N\omega_i\sqrt{L_L C_L}, \quad i=1,2 \tag{3}$$

$$\phi_i^{\mathrm{LH}} = \frac{N}{\omega_i\sqrt{L_L C_L}}, \quad i=1,2 \tag{4}$$

$$Z_{\mathrm{LH}} = \sqrt{\frac{L_L}{C_L}} \tag{5}$$

where N, Z_{LH}, and Z_{RH} are the number of LT TL units, characteristic impedances of LH, and RH TL, respectively. ϕ_i^{RH} and ϕ_i^{LH} are the phase of RH and LH TL at ω_i.

Figure 3 shows the equivalent transmission line modeling of the

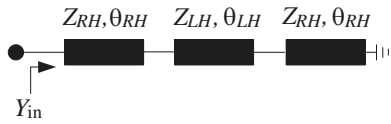

Figure 3. The equivalent transmission model of short stub CRLH.

short stub CRLH. Assuming $Z_{\text{RH}} = Z_{\text{LH}} = Z$, the input admittance of short stub is given as:

$$Y_{\text{in}} = -jZ \tan\left(2\theta_{\text{RH}} + \theta_{\text{LH}}\right) \tag{6}$$

where θ_{RH} and θ_{LH} are electrical lengths of RH and LH TL, respectively. The susceptance slope parameter [29] of the short stub CRLH at a resonance frequency can be found using (6), which is given as:

$$b_i = \frac{\omega_i}{2}\frac{dB}{d\omega}\bigg|_{\omega=\omega_i} = \frac{1}{2Z}\left(2\theta_{\text{RH}} + \theta_{\text{LH}}\right)\text{cosec}^2\left(2\theta_{\text{RH}} + \theta_{\text{LH}}\right) \tag{7}$$

The proposed dual-band admittance inverter (J-inverter) shown in Fig. 1 consists of open stubs and transmission line with characteristics impedance Z_1 and Z_2, respectively. The corresponding electrical lengths are θ_1 and θ_2, which are all defined at frequency f_1. The total $ABCD$ parameter of the proposed dual-band admittance inverter is obtained as (8).

$$\begin{bmatrix} A & B \\ C & D \end{bmatrix}_T = \begin{bmatrix} \cos\theta_2 - \frac{Z_2}{Z_1}\tan\theta_1 \sin\theta_2 & jZ_2 \sin\theta_2 \\ j\frac{1}{Z_2 \sin\theta_2} & \cos\theta_2 - \frac{Z_2}{Z_1}\tan\theta_1 \sin\theta_2 \end{bmatrix} \tag{8}$$

The $ABCD$ parameter of ideal admittance inverter (J-inverter) is expressed as

$$\begin{bmatrix} A & B \\ C & D \end{bmatrix}_J = \begin{bmatrix} 0 & j\dfrac{1}{J} \\ jJ & 0 \end{bmatrix} \tag{9}$$

The dual-band admittance inverter as shown in Fig. 1 is the dual-band quarter-wavelength TL that exhibits the same admittance value and same 90° phase shift at two operating frequencies. For dual-band admittance inverter, the same value of J and phase shift of 90° should be given and evaluated at two designated frequencies (f_1 and f_2). The simultaneous equations for solving the parameters of dual-band inverter are written by equating $ABCD$ parameters of (8) and (9) to satisfy two frequency bands.

$$\cos\theta_2 - \frac{Z_2}{Z_1}\tan\theta_1 \sin\theta_2 = 0 \tag{10}$$

$$\cos(a\theta_2) - \frac{Z_2}{Z_1}\tan(a\theta_1)\sin(a\theta_2) = 0 \tag{11}$$

$$Z_2 \sin\theta_2 = \frac{1}{J} \tag{12}$$

$$Z_2 \sin(a\theta_2) = \frac{1}{J} \tag{13}$$

where a is the frequency ratio (f_2/f_1) between two frequency bands. It is found that the solutions of θ_1 and θ_2 are [30].

$$\theta_1 = \theta_2 = \frac{\pi}{a+1} = \frac{\pi f_1}{f_2 + f_1} \tag{14}$$

The characteristic impedance of transmission line and open stubs are obtained by solving (10) and (12), respectively.

$$Z_2 = \frac{1}{J\sin\theta_2} \tag{15}$$

$$Z_1 = \frac{\tan\theta_1}{J\cos\theta_2} \tag{16}$$

For simplicity, the resonators at each stage are selected same. Assuming the 3-dB FBWs as Δ_1 and Δ_2 at two operating frequencies f_1 and f_2, the admittance inverters between resonators are determined as:

$$(J_{i,i+1})_1 = (J_{i,i+1})_2, \quad i = 1, 2, \cdots, n \tag{17}$$

$$J_{i,i+1} = \Delta_1\sqrt{\frac{b_1^2}{g_i g_{i+1}}} = \Delta_1\sqrt{\frac{b_2^2}{g_i g_{i+1}}} \tag{18}$$

where b_1 and b_2 are the susceptance slope parameters of resonators at two operating frequencies, which are calculated from (7).

3. SIMULATION AND MEASUREMENT

In order to validate of the proposed structure, simulation and experiment were performed by constructing the second order Chebyshev-type dual-band BPF on a substrate RT/Duroid-5880 made by Rogers Corporation with a dielectric constant (ε_r) of 2.2 and thickness (h) of 31 mils. The center frequencies of the dual-band BPF are specified at 2.4 GHz and 5.2 GHz with the 3-dB FBWs of $\Delta_1 = 57\%$ and $\Delta_2 = 21\%$, respectively. The prototype element values of Chebyshve low pass filter with the passband ripple of 0.01 dB and $n = 2$ are $g_0 = 1$, $g_1 = 0.4488$, $g_2 = 0.4077$ and $g_3 = 1.1007$, respectively. With given specification, the calculated values of slope parameters

of CRLH resonators are $b_1 = 0.0157$ mhos and $b_2 = 0.0471$ mhos. The element values of the short stub CRLH are given in Table 1. The inductance values of the CRLH TL are implemented with short circuited high impedance TL stubs. The designed parameters of admittance inverter are $\theta_1 = \theta_2 = 56.84°$, $Z_1 = 134.4\,\Omega$, $Z_2 = 57.7\,\Omega$ at 2.4 GHz respectively.

Figure 4 shows the simulated and measured results of the proposed broad-bandwidth dual-band BPF. Referring to this figure, it is seen that the measurement result shows a good agreement with the simulated one. The measured insertion losses are 0.28 dB and 0.46 dB with 3-dB FBWs of 50.24% and 20.20% at two passbands, respectively. The measured return loss is less than 18.4 dB and 21.4 dB in the first and second passbands, respectively. The attenuation is larger than 20 dB from 3.51 to 4.31 GHz between two passbands. The comparison between the simulated and measured performances of the proposed BPF is summarized in Table 2. Table 3 summarizes the comparison of the proposed filter with other reported dual-band BPFs. Fig. 5 shows the photograph of fabricated broad-bandwidth dual-band BPF.

Table 1. Component values of short stub CRLH.

$N = 2$	Calculation	EM Simulation	Measurement
C_L (PF)	3.4553	3.40	3.40
$2C_L$ (PF)	6.9106	6.80 short stub	6.80 short stub
L_L (NH)	8.6383	53.90°, 133 Ω@f_1	53.90°, 133 Ω@f_1
$2\theta_{\mathrm{RH}}$@f_1 (deg)	133.98°@f_1	112.64°@f_1	112.64°@f_1

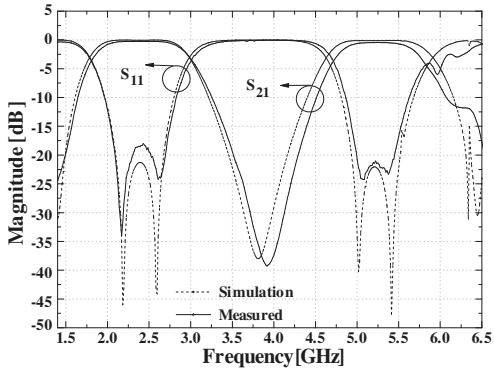

Figure 4. Simulated and measured result.

Figure 5. The photograph of the fabricated broad-bandwidth dual-band bandpass filter.

Table 2. Simulation and measured performance.

Center Freq	Simulation			Measurement		
[GHz]	S_{11} [dB]	S_{21} [dB]	3-dBFBM [%]	S_{11} [dB]	S_{21} [dB]	3-dBFBM [%]
2.4	−21.30	−0.06	50.20	−18.40	−0.28	50.24
5.2	−22.10	−0.14	24.80	−21.46	−0.46	20.20

Table 3. Performance comparison with other proposed broadband dual-band filters.

References	[15]	[16]	[17]	[18]	[25]	**This work**
Substrate height (mm)/ε_r	0.762/3.38	0.508/2.2	0.787/2.2	1.57/6.15	1.27/10.2	**0.787/2.2**
1st/2nd Passbands (GHz)	2.40/5.20	3.43/5.95	2.40/5.20	2.40/5.20	1.0/1.90	**2.40/5.20**
Return Loss (dB)	20/20	12/12	20/15	12/12	16.7/21.8	**18.14/21.46**
Insertion Loss (dB)	0.8/0.9	0.7/1	0.89/0.9	0.75/1	0.939/0.935	**0.28/0.46**
3-dB FBW (%)	48/18	31/13	45/10	35/18	29.8/17.3	**50.24/20.20**

4. CONCLUSION

In this paper, a novel design of dual-band bandpass filter with a broad bandwidth is demonstrated using the dual-band characteristics of composite right/left handed meta-material. The coupling between the resonators required for the dual-band bandpass filter has

been implemented by dual-band admittance inverters. Simple design equations are presented to design broad-bandwidth dual-band bandpass filter. Experiment has been provided to verify the theoretical and simulation predictions. The proposed dual-band filter offers low insertion losses in both of the passbands and expected to be suitable for WLANs applications.

REFERENCES

1. Miyake, H., S. Kitazawa, T. Ishizaki, Y. Yamada, and Y. Nagatomi, "A miniaturized monolithic dual band filter using ceramic lamination technology for dual-mode portable telephones," *IEEE MTT-S Int. Microwave Symposium Dig.*, 789–792, 1997.
2. Abu-Hundrouss, A. M. and M. J. Lancaster, "Design of multiple-band microwave filters using cascaded filter elements," *Journal of Electromagnetic Waves and Applications*, Vol. 23, No. 16, 2109–2118, 2009.
3. Hung, C. Y., R. Y. Yang, and Y. L. Lin, "A simple method to design a compact and high performance dual-band bandpass filter for GSM and WLAN," *Progress In Electromagnetics Research C*, Vol. 13, 187–193, 2010.
4. Yang, R. Y., K. Hon, and C. Y. Hung, "Design of dual-band bandpass filters using a dual-feeding structure and embedded uniform impedance resoantors", *Progress In Electromagnetics Research*, Vol. 105, 93–102, 2010.
5. Guan, X., Z. Ma, P. Chai, Y. Kobayashi, T. Anada, and G. Hagiwara, "Synthesis of dual-band bandpass filter using successive frequency transformations and circuit conversions," *IEEE Microw. Wireless Comp. Letters*, Vol. 16, No. 3, 110–112, Mar. 2006.
6. Zhang, Y. P. and M. Sun, "Dual-band microstrip bandpass filter using stepped impedance resonators with new coupling scheme," *IEEE Trans. on Microwave Theory and Tech.*, Vol. 54, No. 10, 3779–3785, Oct. 2006.
7. Weng, M. H., C. H. Kao and Y. C. Chang, "A compact dual-band bandpass filter with high band selectivity using cross-coupled asymmetric SIRs for WLANs," *Journal of Electromagnetic Waves and Applications*, Vol. 24, No. 2/3, 161–168, 2010.
8. Alkanhal, M. A. S., "Dual-band bandpass filters using inverted stepped-impedance resonators," *Journal of Electromagnetic Waves and Applications*, Vol. 23, No. 8/9, 1211–1220, 2009.

9. Chiou, Y. C., P. S. Yang, J. T. Kuo, and C. Y. Wu, "Transmission zero design graph for dual-mode dual-band filter with periodic stepped impedance ring resonator," *Progress In Electromagnetics Research*, Vol. 108, 23–36, 2010.
10. Xiao, J. K. and H. F. Huang, "New dual-band bandpass filter with compact SIR structure," *Progress In Electromagnetics Research Letters*, Vol. 18, 125–134, 2010.
11. Sun, X. and E. L. Tan, "A novel dual-band bandpass filter using generalized trisection stepped impedance resonator with improved out of band performance," *Progress In Electromagnetics Research Letters*, Vol. 21, 31–40, 2011.
12. Wang, J. P., L. Wang, Y. X. Guo and Y. X. Wang, "Miniaturized dual-mode bandpass filter with controllable harmonic response for dual-band applications," *Journal of Electromagnetic Waves and Applications*, Vol. 23, No. 11/12, 1525–1533, 2009.
13. Velazquez-Ahumada, M. D. C., J. Martel, F. Medina, and F. Mesa, "Application of stub-loaded folded stepped impedance resonators to dual band filter design," *Progress In Electromagnetics Research*, Vol. 107, 107–124, 2010.
14. Wu, G. L., W. Mu, X. W. Dai, and Y. C. Jia, "Design of novel dual-band bandpass filter with microstrip meander-loop resonator and CSRR DGS," *Progress In Electromagnetics Research*, Vol. 78, 17–24, 2008.
15. Chin, K. S. and J. H. Yeh, "Dual-wideband bandpass filter using short-circuited stepped impedance resonators," *IEEE Microw. Wireless Comp. Letters*, Vol. 19, No. 3, 155–157, Mar. 2009.
16. Wu, Y. L., C. Lia, and X. Z. Xiong, "A dual-wideband bandpass filter based on E-shaped microstrip SIR with improved upper-stopband performance," *Progress In Electromagnetics Research*, Vol. 108, 141–153, 2010.
17. Weng, M. H., S. K. Liu, H. W. Wu, and C. H. Hung, "A dual-band bandpass filter having wide and narrow bands simultaneously using multilayered stepped impedance resonators," *Progress In Electromagnetics Research Letters*, Vol. 13, 139–147, 2010.
18. Wang, X. H., B. Z. Wang, and K. J. Chen, "Compact broadband dual-band bandpass filters using slotted ground structures," *Progress In Electromagnetics Research*, Vol. 82, 151–166, 2008.
19. Lin, I., M. DeVincentis, C. Caloz, and T. Itoh, "Arbitrary dual-band components using composite right/left handed transmission lines," *IEEE Trans. on Microwave Theory and Tech.*, Vol. 52, No. 4, 1142–1149, Apr. 2004.

20. Jimenez-Martin, J. L., V. Gonzalez-Posadas, J. E. Gonzalez-Garcia, F. J. Arqures-Orobon, L. E. Garcia-Munoz, and D. Segovia-Vargas, "Dual-band high efficiency class CE power amplifier based on CRLH diplexer," *Progress In Electromagnetics Research*, Vol. 97, 217–240, 2009.
21. Huang, J. Q. and Q. X. Chu, "Compact UWB band-pass filter utilizing modified composite right/left-handed structure with cross coupling," *Progress In Electromagnetics Research*, Vol. 107, 179–186, 2010.
22. Chou, T. C., M. H. Tsai, and C. Y. Chen, "A low insertion loss and high selectivity UWB bandpass filter using composite right/left handed material," *Progress In Electromagnetics Research C*, Vol. 17, 163–172, 2010.
23. Liu, X., C. Li, and F. Li, "Novel dual-band microwave components using composite right/left handed transmission lines," *International Workshop on Metamaterial*, 347–350, Nov. 2008.
24. Jang, G. and S. Kahang, "Design of a dual-band metamaterial bandpass filter using zeroth order resonance," *Progress In Electromagnetics Research C*, Vol. 12, 149–162, 2010.
25. Tseng, C.-H. and T. Itoh, "Dual-band bandpass and bandstop filters using composite right/left handed metamaterial transmission line," *IEEE MTT-S Int. Microwave Symposium Dig.*, 931–934, Jun. 2006.
26. Lin, Y. S., W. C. Ku, C. H. Wang, and C. H. Chen, "Wideband coplanar-waveguide bandpass filter with good stopband rejection," *IEEE Microw. Wireless Comp. Letters*, Vol. 14, No. 9, 422–424, Sep. 2004.
27. Deng, H. W., Y. J. Zhao, L. Zhang, X. S. Zhang, and W. Zhao, "Compact wideband bandpass filter with quadruple-mode stub loaded resonator," *Progress In Electromagnetics Research Letters*, Vol. 17, 125–132, 2010.
28. Caloz, C. and T. Itoh, *Electromagnetic Metamaterials: Transmission lines Theory and Microwave Applications*, Wiley, 2006.
29. Matthaei, G., L. Young, and E. M. T. Jones, *Microwave Filters, Impedance-matching Networks, and Coupling Structure*, McGraw-Hill Book Co., New York, NY, 1964.
30. Tsai, C. M., H. M. Lee, and C. C. Tsai, "Planar filter design with fully controllable second passband," *IEEE Trans. on Microwave Theory and Tech.*, Vol. 53, No. 11, 3429–3438, Nov. 2005.